J. Biochem. 132, 345–352 (2002)

Ca^{2+}- and S1-Induced Movement of Troponin T on Mutant Thin Filaments Reconstituted with Functionally Deficient Mutant Tropomyosin[1]

Chieko Kimura,[*] Kayo Maeda,[†] Hong Hai,[*] and Masao Miki[*,2]

[*]*Department of Applied Chemistry and Biotechnology, Fukui University, 3-9-1 Bunkyo, Fukui 910-8507; and* [†]*Riken Harima Institute at Spring8, Mikazuki-cho, Sayo, Hyogo, 679-5143*

Received May 15, 2002; accepted June 18, 2002

The deletion mutant (D234Tm) of rabbit skeletal muscle α-tropomyosin, in which internal actin-binding pseudo-repeats 2, 3, and 4 are missing, inhibits the thin filament activated myosin-ATPase activity whether Ca^{2+} ion is present or not [Landis *et al.* (1997) *J. Biol. Chem.* 272, 14051–14056]. Fluorescence resonance energy transfer (FRET) showed substantial changes in distances between Cys-60 or 250 of troponin T (TnT) and Gln-41 or Cys-374 of actin on wild-type thin filaments corresponding to three states of thin filaments [Kimura *et al.* (2002) *J. Biochem.* 132, 93–102]. Troponin T movement on mutant thin filaments reconstituted with D234Tm was compared with that on wild-type thin filaments to understand from which the functional deficiency of mutant thin filaments derives. The Ca^{2+}-induced changes in distances between Cys-250 of TnT and Gln-41 or Cys-374 of F-actin were smaller on mutant thin filaments than on wild-type thin filaments. On the other hand, the distances between Cys-60 of TnT and Gln-41 or Cys-374 of F-actin on mutant thin filaments did not change at all regardless of whether Ca^{2+} was present. Thus, FRET showed that the Ca^{2+}-induced movement of TnT was severely impaired on mutant thin filaments. The rigor binding of myosin subfragment 1 (S1) increased the distances when the thin filaments were fully decorated with S1 in the presence and absence of Ca^{2+}. However, plots of the extent of S1-incuced movement of TnT against molar ratio of S1 to actin in the presence and absence of Ca^{2+} showed that the S1-induced movement of TnT was also impaired on mutant thin filaments. The deficiency of TnT movement on mutant thin filaments causes the altered S1-induced movement of TnI, and mutant thin filaments consequently fail to activate the myosin-ATPase activity even in the presence of Ca^{2+}.

Key words: D234Tm, FRET, regulation mechanism, thin filament, troponin T.

In striated muscle, the interaction between actin and myosin is regulated by tropomyosin (Tm) and troponin (Tn) on the actin filament in response to changes of intracellular Ca^{2+} concentration (*1*). The Tm molecule contains seven quasiequivalent regions, each of which contains a pair of putative actin-binding motifs. Tn consists of three different subunits, troponin C (TnC), troponin I (TnI), and troponin T (TnT). The globular part of troponin composed of TnC and TnI binds to tropomyosin near Cys-190 (residues: 150–180) (*2*), and the elongated part composed of TnT covers over an extensive region of the COOH-terminal half of tropomyosin (*3*). TnI alone inhibits the actomyosin ATPase, and the inhibition is removed on adding TnC irrespective of Ca^{2+} concentration. TnT is required for full Ca^{2+}-regulation of the ATPase activity of a reconstituted system (*3*). Numerous studies have characterized the interaction between the thin filament proteins to deduce how the Ca^{2+}-triggering signal is propagated from TnC to the rest of a thin filament [see reviews (*4, 5*)].

Fluorescence resonance energy transfer (FRET) has been extensively used for structural studies of muscle proteins (*6, 7*). This method is especially valuable for detecting a small conformational change, since the transfer efficiency is a function of the inverse of the sixth power of the distance between probes. Furthermore, fluorescence donor and ac-

[1] This study was supported by Special Coordination Funds of the Ministry of Education, Culture, Sports, Science and Technology, the Japanese Government.

[2] To whom correspondence should be addressed. Tel: +81-776-27-8786, Fax: +81-776-27-8747, E-mail: masao@acbio2.acbio.fukui-u.ac.jp

Abbreviations: 3D-EM, three-dimensional image reconstruction of electron micrographs; DABMI, 4-dimethyl-aminophenylazophenyl 4′-maleimide; FLC, fluorescein cadaverine; FRET, fluorescence resonance energy transfer; IAEDANS, 5-(2-iodoacetylaminoethyl)aminonaphthalene 1-sulfonic acid; S1, myosin subfragment 1; Tm, tropomyosin; Tn, troponin; TnC, troponin C; TnI, troponin I; TnT, troponin T; TnT 25k, a mutant rabbit skeletal β-troponin T 25-kDa fragment which lacks the N-terminal region 1–58; AEDANS-60-TnT, TnT 25k (E60C) in which the second (60th in the full length TnT) glutamate was replaced with cysteine and labeled with IAEDANS; AEDANS-250-TnT, TnT 25k (S250C) in which 192nd (250th in full length TnT) serine was replaced with cysteine and labeled with IAEDANS; AEDANS-60-Tn, the reconstituted troponin complex using AEDANS-60-TnT; AEDANS-250-Tn, the reconstituted Tn complex using AEDANS-250-TnT; D234Tm, rabbit Ala-Ser-α-tropomyosin Δ (49–167) which was expressed by *Escherichia coli*.

ceptor molecules are specifically labeled so that the assignment of the conformational change is direct. Using this method, several attempts were made to detect conformational changes of Tm and Tn on the reconstituted thin filament. FRET between probes attached to Tm (at positions 87 and 190) and actin (at positions 41, 61, 374, and the nucleotide binding site) showed no significant Ca^{2+}-induced movement of Tm (*8*). On the other hand, FRET between probes attached to TnI and actin demonstrated a significant Ca^{2+}-induced movement of TnI (*9–12*), and also S1-induced movement of TnI (*13, 14*). Thus, FRET demonstrated that TnI moves on a thin filament corresponding to three states of the thin filament.

D234Tm, in which three of seven repeats (49–167 amino acid residues) have been deleted, retains the ability to bind normally to actin and Tn, but it inhibits actomyosin MgATPase and filament sliding *in vitro*, which is not reversed by Ca^{2+} and Tn (*15*). Using mutant D234Tm, Rosol *et al.* (*16*) reported that 3D-EM showed no difference in the Ca^{2+}-induced conformational changes between thin filaments containing wild-type Tm and those containing mutant D234Tm. They concluded that mutation did not affect normal Tm movement induced by Ca^{2+} and Tn. They suggested the importance of the S1-induced conformational change (open state) for active acto-S1 interaction, but they did not detect any difference in the S1-induced conformational change between wild-type and mutant thin filaments. On the other hand, Ca^{2+}- and S1-induced movements of TnI and D234Tm on mutant thin filaments reconstituted with D234Tm were examined by FRET (*14*). Although no significant movement of D234Tm or wild-type Tm was detected, the Ca^{2+}-induced movement of TnI was shown to occur on mutant thin filaments normally as on wild-type thin filaments. However, plots of the extent of S1-induced conformational change *vs.* molar ratio of S1 to actin showed that the curve for wild-type thin filaments is hyperbolic, whereas that for mutant thin filaments is sigmoidal in the presence of Ca^{2+}. In the absence of Ca^{2+}, curves are sigmoidal for both wild-type and mutant thin filaments. These results suggest that a transition from closed state to open state in the presence of ATP is strongly depressed in mutant thin filaments, which results in the inhibition of acto-myosin ATPase even in the presence of Ca^{2+}.

In the preceding paper (*17*), single thiol mutants of rabbit skeletal β-type TnT 25-kDa fragment were generated in which a single cysteine residue was introduced at position 60 in the N-terminal region or position 250 in the C-terminal region. FRET between these points of TnT and Cys-374 or Gln-41 of actin on reconstituted thin filaments in the presence or absence of Ca^{2+} ion or S1 demonstrated that not only TnI but also TnT change their positions on the thin filament corresponding to three states of thin filaments. FRET also showed that the curve of S1-induced movement of TnT *vs.* molar ratio of S1 to actin was hyperbolic in the presence of Ca^{2+}, but sigmoidal in the absence of Ca^{2+}. In the present study, Ca^{2+}- and S1-induced movements of TnT on functionally deficient mutant thin filaments reconstituted with D234Tm were measured by FRET in order to determine what conformational changes are critical for regulation mechanism.

MATERIALS AND METHODS

Reagents—Phalloidin from *Amanita phalloides* was purchased from Sigma. IAEDANS, DABMI and FLC were purchased from Molecular Probes. BCA Protein assay reagent was from Pierce Chemicals. All other chemicals were of analytical grade.

Protein Preparations—Actin, S1, and Tn were prepared from rabbit skeletal muscle, and α-Tm was extracted from rabbit hearts as reported previously (*9*). Microbial transglutaminase was a generous gift from Food Research and Development Laboratories, Ajinomoto. Single cysteine TnT25k mutants (E60C and S250C) were prepared as reported in the preceding paper (*17*). The deletion mutant Tm (D234Tm), in which internal actin-binding pseudo-repeats 2, 3, 4 are missing, was prepared as reported previously (*14*). Protein concentrations were determined by use of absorption coefficients of A_{290} = 0.63 $(mg/ml)^{-1}$ cm^{-1} for G-actin, A_{280} = 0.75 $(mg/ml)^{-1}$ cm^{-1} for S1, 0.31 $(mg/ml)^{-1}$ cm^{-1} for Tm, 1.024 × 10^4 M^{-1} cm^{-1} for D234Tm, 0.45 $(mg/ml)^{-1}$ cm^{-1} for Tn and 0.67 $(mg/ml)^{-1}$ cm^{-1} for TnT25k. The concentrations of labeled proteins were measured at 540 nm with the BCA protein assay reagent with the respective unlabeled proteins as standards. Relative molecular masses of 43,000 for actin, 115,000 for S1, 66,000 for Tm, 37,700 for D234Tm, 69,000 for Tn, 25,000 for TnT25k mutants, and 38,000 for transglutaminase were used.

Labeling of Proteins—Actin was labeled at Gln-41 with FLC or at Cys-374 with DABMI as described previously (*12*). TnT25k mutants were labeled with IAEDANS, and reconstitution of ternary Tn complexes with AEDANS-labeled TnT25k mutants was carried out as reported in the preceding paper (*17*)

Spectroscopic Measurements—Absorption was measured with a Hitachi U2000 spectrophotometer. Steady-state fluorescence was measured at 20°C with a Perkin Elmer LS50B fluorometer. The absorption coefficients of 24,800 M^{-1} cm^{-1} at 460 nm for DABMI (*18*), 75,500 M^{-1} cm^{-1} at 493 nm for FLC (*19*), and 6,100 M^{-1} cm^{-1} at 334 nm for IAEDANS (*20*) were used for the determination of labeling ratios. The typical labeling ratios were 0.96 for DAB-F-actin, 1.0 for FLC-F-actin, 0.75 for AEDANS-250-Tn and 0.74 for AEDANS-60-Tn.

Fluorescence Resonance Energy Transfer—The efficiency E of resonance energy transfer between probes was determined by measuring the fluorescence intensity of the donor both in the presence (F_{DA}) and absence (F_{D0}) of the acceptor as given by

$$E = 1 - F_{DA}/F_{D0} \quad (1)$$

The efficiency is related to the distance (R) between donor and acceptor, and Förster's critical distance (R_0) at which the transfer efficiency is equal to 50% [see reviews (*6, 7*)]

$$E = R_0^6/(R^6 + R_0^6) \quad (2)$$

R_0 can be obtained (in nm) with

$$R_0^6 = (8.79 \times 10^{-11})\, n^{-4}\, \kappa^2\, Q_0 J \quad (3)$$

where n is the refractive index of the medium, taken as 1.4, κ^2 is the orientation factor, Q_0 is the quantum yield of the donor in the absence of the acceptor, and J is the spectral overlap integral between the donor emission $F_D(\lambda)$ and ac-

ceptor absorption $\varepsilon_A(\lambda)$ spectra defined by

$$J = \int F_D(\lambda)\, \varepsilon_A(\lambda)\, \lambda^4\, d\lambda / \int F_D(\lambda)\, d\lambda \quad (4)$$

The quantum yield was determined by a comparative method using quinine sulfate in 1 M H_2SO_4 as the standard, which has an absolute quantum yield of 0.70 (*21*). The value of κ^2 was taken as 2/3 for calculation of distances both in the presence and absence of Ca^{2+} and/or S1, as mentioned in the preceding paper (*17*). The decrease of the fluorescence intensity due to inner filter effects was corrected with

$$F_{corr} = F_{obs} \times 10^{(A_{ex}+A_{em})/2} \quad (5)$$

where A_{ex} and A_{em} are the absorption of the sample at the excitation and emission wavelengths, respectively.

RESULTS

The AEDANS moiety bound to Cys-60 or Cys-250 of mutant 25-kDa fragments of β-TnT was used as the energy donor, while FLC or DABMI attached to Gln-41 or Cys-374 of actin, respectively, was used as the energy transfer acceptor. ATPase measurements indicated that neither the mutation nor the labeling of AEDANS affected the regulatory activity of TnT, as shown in the preceding paper (*17*). The D234Tm and Tn complex inhibited actoS1-MgATPase activity irrespective of the presence of Ca^{2+} ions, as reported previously (*14*).

FRET between Cys-60 or Cys-250 of TnT and Gln-41 or Cys-374 of F-Actin on Mutant Thin Filaments Reconstituted with D234Tm in the Presence and Absence of Ca^{2+}—Figure 1 shows the fluorescence spectra of AEDANS-250-Tn on mutant thin filaments reconstituted with D234Tm in the presence (curves 2 and 5) and absence (curves 1 and 4) of an acceptor (DABMI bound to F-actin). The solvent conditions were 30 mM KCl, 20 mM Tris-HCl (pH 7.6), 2 mM $MgCl_2$, 0.1 mM ATP, 1 mM NaN_3 (buffer F) and 50 μM $CaCl_2$ for the $+Ca^{2+}$ state (curves 1 and 2) or 1 mM EGTA for the $-Ca^{2+}$ state (curves 4 and 5) at 20°C.

In the absence of acceptor, the donor fluorescence was slightly smaller for the $+Ca^{2+}$ state than for the $-Ca^{2+}$ state; but in the presence of the acceptor, it was greater for the $+Ca^{2+}$ state than for the $-Ca^{2+}$ state. The result indicated that the transfer efficiency between AEDANS-250-Tn and DAB-F-actin was greater in the absence than in the presence of Ca^{2+}. The Ca^{2+}-dependency of donor fluorescence spectra for the mutant thin filament was smaller than that reported in the preceding paper for the wild-type thin filament (*17*). Surprisingly, however, in the case of AEDANS-60-Tn, the donor fluorescence spectra in the presence and absence of acceptor did not depend on Ca^{2+} concentration for mutant thin filaments, although they showed strong dependency on Ca^{2+} concentration for wild-type thin filaments (*17*). The results indicate that the C-terminal region of TnT moves less and the N-terminal region does not move at all on mutant thin filaments in response to Ca^{2+} concentrations. FRET between FLC attached to Gln-41 on F-actin and AEDANS-60-Tn or AEDANS-250-Tn was measured. The fluorescence spectra of AEDANS-60-Tn and AEDANS-250-Tn were measured under the same solvent conditions as in Fig. 1 but with FLC bound to Gln-41 as the acceptor instead of DABMI bound to Cys-374 of actin. FRET between FLC-F-actin and AEDANS-60-Tn or AEDANS-250-Tn showed a similar manner of transfer efficiency to the case of DAB-F-actin.

The overlap integral, J, was determined to be 6.52×10^{14} M^{-1} cm^{-1} nm^4 for the AEDANS-60-Tn/DAB-F-actin pair, 6.64×10^{14} M^{-1} cm^{-1} nm^4 for AEDANS-250-Tn/DAB-F-actin, 16.6×10^{14} M^{-1} cm^{-1} nm^4 for AEDANS-60-Tn/FLC-F-actin, and 17.4×10^{14} M^{-1} cm^{-1} nm^4 for AEDANS-250-Tn/FLC-F-actin. The quantum yield, Q_0, of AEDANS-60-Tn was 0.30 irrespective of Ca^{2+} concentration, and Q_0 of AEDANS-250-Tn was 0.34 for $+Ca^{2+}$ and 0.37 for $-Ca^{2+}$. By taking $n = 1.4$ and $\kappa^2 = 2/3$, the Förster's critical distance, R_0, for the AEDANS-60-Tn/DAB-F-actin pair was determined to be 37.9 Å irrespective of Ca^{2+} concentration. R_0 for the AEDANS-250-Tn/DAB-F-actin pair was determined to be 38.9 Å for $+Ca^{2+}$ and 39.4 Å for $-Ca^{2+}$. R_0 for the AEDANS-60-Tn/FLC-F-actin pair was determined to be 44.3 Å irre-

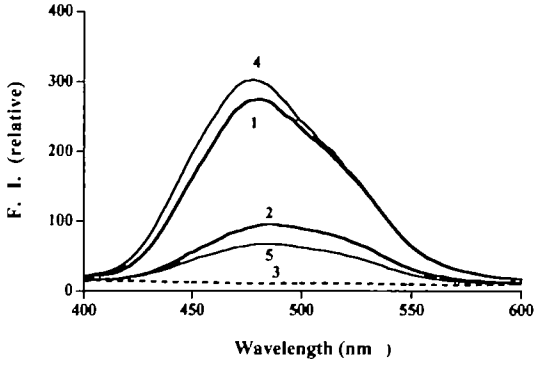

Fig. 1. **Fluorescence spectra of AEDANS bound to Cys-250 of TnT on mutant thin filaments in the presence and absence of acceptor (DABMI bound to Cys-374 of actin).** (1) F-actin/D234Tm/AEDANS-250-Tn/$+Ca^{2+}$ (2) DAB-F-actin/D234Tm/AEDANS-250-Tn/$+Ca^{2+}$ (3) DAB-F-actin/D234Tm/Tn/$\pm Ca^{2+}$ (4) F-actin/D234Tm/AEDANS-250-Tn/$-Ca^{2+}$ (5) DAB-F-actin/D234Tm/AEDANS-250-Tn/$-Ca^{2+}$. Spectra were measured at 20°C in 30 mM KCl, 2 mM $MgCl_2$, 20 mM Tris-HCl (pH 7.6), 1 mM NaN_3 (buffer F), and 50 μM $CaCl_2$ for the $+Ca^{2+}$ state or 1 mM EGTA for the $-Ca^{2+}$ state. Concentrations of actin, D234Tm, and Tn were 0.2, 0.044, and 0.042 mg/ml, respectively. Excitation was at 340 nm.

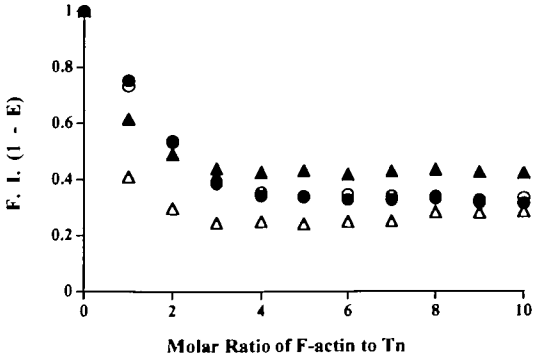

Fig. 2. **Relative fluorescence intensities of AEDANS bound to Cys-60 (●, ○) and Cys-250 (▲, △) of TnT in the Tn-D234Tm complex *vs.* molar ratio of DAB-F-actin.** Values were obtained in buffer F and 50 μM $CaCl_2$ for the $+Ca^{2+}$ state (●, ▲) or 1 mM EGTA for the $-Ca^{2+}$ state (○, △) at 20°C, after correction of the inner filter effects according to Eq. 5. Concentrations of AEDANS-Tn and D234Tm were 0.042 and 0.044 mg/ml, respectively. Excitation was at 340 nm and emission was measured at 490 nm.

spective of Ca^{2+} concentration. R_0 for the AEDANS-250-Tn/FLC-F-actin pair was determined to be 45.6 Å for $+Ca^{2+}$ and 46.3 Å for $-Ca^{2+}$.

To obtain more quantitative data on the transfer efficiency, the ratio of donor fluorescence quenching was measured by titrating AEDANS-Tn/D234Tm with DAB-F-actin in the presence (buffer F + 50 μM $CaCl_2$) and absence of Ca^{2+} ions (buffer F + 1 mM EGTA) at 20°C (Fig. 2). To correct the fluorescence intensity change of AEDANS-Tn upon binding to an F-actin filament, the same amount of non-labeled F-actin was added to the AEDANS-Tn/D234Tm as reference, and the ratio of these fluorescence intensities was taken as the relative fluorescence intensity. The apparent decrease of the fluorescence intensity due to inner filter effects arising from the absorbance of DAB-F-actin was corrected according to Eq. 5. The relative fluorescence intensity decreased gradually in the actin/Tn molar ratio range up to 4 and became almost constant in the range over 4 on the mutant thin filament reconstituted with D234Tm, as compared with a critical ratio of 7 on the wild-type thin filament reconstituted with full-length Tm. From the saturation points, the apparent energy transfer efficiencies were calculated to be 0.70 ± 0.01 irrespective of Ca^{2+} concentration in the case of AEDANS-60-Tn, and 0.60 ± 0.01 for the $+Ca^{2+}$ state and 0.79 ± 0.02 for the $-Ca^{2+}$ state in the case of AEDANS-250-Tn. These transfer efficiencies correspond to distances of 33.0 ± 0.3 Å in the case of AEDANS-60-Tn, and 36.4 ± 0.3 Å for the $+Ca^{2+}$ state and 31.5 ± 0.6 Å for the $-Ca^{2+}$ state in the case of AEDANS-250-Tn.

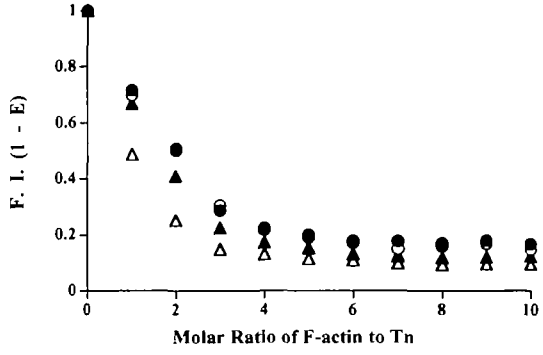

Fig. 3. **Relative fluorescence intensities of AEDANS bound to Cys-60 (●, ○) and Cys-250 (▲, △) of TnT in the Tn-D234Tm complex *vs.* molar ratio of FLC-F-actin.** Values were obtained in buffer F and 50 μM $CaCl_2$ for the $+Ca^{2+}$ state (●, ▲) or 1 mM EGTA for the $-Ca^{2+}$ state (○, △) at 20°C, after correction of the inner filter effects according to Eq. 5. Concentrations of AEDANS-Tn and D234Tm were 0.042 and 0.044 mg/ml, respectively. Excitation was at 340 nm and emission was measured at 460 nm.

AEDANS-60-Tn/D234Tm and AEDANS-250-Tn/D234Tm were also titrated with FLC-F-actin in the same way as DAB-F-actin (Fig. 3). Fluorescence intensity was measured at 460 nm, where no contribution of the acceptor-fluorescence from FLC occurs. The energy transfer efficiencies obtained were 0.82 ± 0.01 irrespective of Ca^{2+} concentration in the case of AEDANS-60-Tn, and 0.85 ± 0.01 and 0.90 ± 0.01 in the case of AEDANS-250-Tn for the $+Ca^{2+}$ and $-Ca^{2+}$ states, respectively. These transfer efficiencies correspond to distances of 34.2 ± 0.4 Å in the case of AEDANS-60-Tn, and 34.2 ± 0.5 Å and 31.9 ± 0.6 Å for the $+Ca^{2+}$ and $-Ca^{2+}$ state, respectively in the case of AEDANS-250-Tn.

Effects of S1 Binding on FRET between AEDANS-60-Tn or AEDANS-250-Tn and FLC- or DAB-F-Actin on Mutant Thin Filaments—Fluorescence spectra of AEDANS bound to Cys-60 or Cys-250 of TnT on reconstituted thin filaments were measured in the presence of S1, using DABMI bound to actin as the energy acceptor. The solvent conditions were buffer F + 50 μM $CaCl_2$ for the $+Ca^{2+}$ state and buffer F + 1 mM EGTA for the $-Ca^{2+}$ state at 20°C. In the absence of an acceptor, the donor fluorescence intensities decreased upon addition of S1 (1/3 mole ratio to actin) for the $-Ca^{2+}$ state but did not change appreciably for the $+Ca^{2+}$ state. In the presence of an acceptor, however, the addition of S1 increased the donor fluorescence intensity significantly for both the $+Ca^{2+}$ and $-Ca^{2+}$ states. The results suggest that rigor S1 binding induced a greater movement of TnT on mutant thin filaments, as was also observed for wild-type thin filaments (*17*). The addition of ATP (1 mM) reversed the changes in FRET induced by rigor S1 binding; and after ATP had been consumed by hydrolysis, the changes in

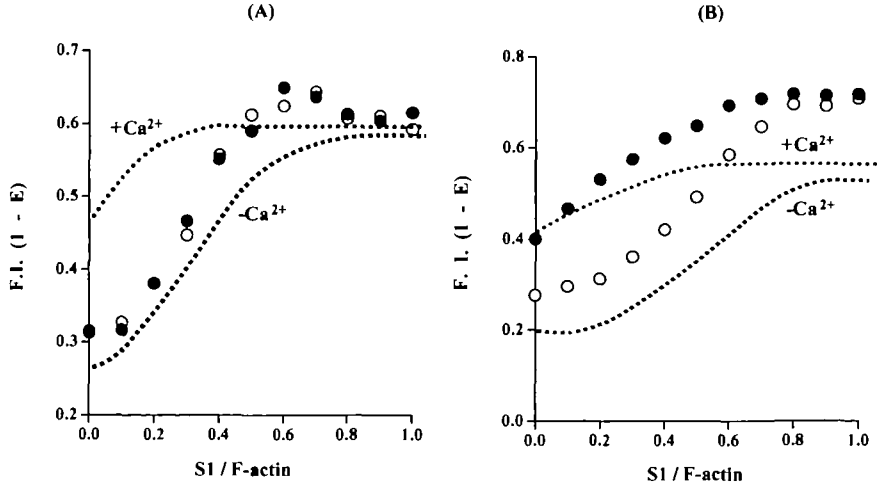

Fig. 4. **Relative fluorescence intensities (1 – *E*) of AEDANS bound to Cys-60 (A) and Cys-250 (B) of TnT on mutant thin filaments *vs.* molar ratios of S1 to actin.** Resonance energy acceptor was DABMI, which was attached to Cys-374 of actin. Values were obtained in buffer F and 50 μM $CaCl_2$ for the $+Ca^{2+}$ state (●) or 1 mM EGTA for the $-Ca^{2+}$ state (○) at 20°C. A small volume of concentrated S1 solution was added stepwise. For the correction of dilution effects, the sample containing of non acceptor-labeled F-actin instead of DAB-F-actin was used as the reference, and the ratio of fluorescence intensities was taken. Concentrations of F-actin, D234Tm, and Tn were 0.23, 0.044, and 0.042 mg/ml, respectively. Fluorescence measurements were carried out after hydrolysis of contaminant ATP (less than 10 μM). Excitation was at 340 nm and emission was measured at 490 nm. Broken lines are the transition curves with wild-type thin filaments instead of mutant thin filaments measured in the preceding paper (*17*).

FRET were again observed.

To obtain more quantitative data on the S1-induced conformational change, changes in the FRET efficiency between AEDANS-60-Tn or AEDANS-250-Tn and D234-Tm/DAB-F-actin were measured by the addition of various amounts of S1 in the presence and absence of Ca^{2+} (Fig. 4). To correct for the dilution effects and fluorescence changes of AEDANS-Tn induced by the addition of S1, the same amounts of S1 were added to the AEDANS-Tn/D234Tm/F-actin as a reference, and the ratios of these fluorescence intensities at 490 nm were taken as the relative fluorescence intensity. To avoid the scattering effects caused by the addition of S1, the non-fluorescent samples of Tn/Tm/DAB-F-actin were prepared under the same solvent conditions as FRET samples, and the same amounts of S1 were added. The scattered light of these non-fluorescent samples was then measured under the same experimental conditions as the FRET samples, and the intensities were subtracted from the fluorescence intensities of FRET samples. The extent of the S1-induced conformational change increased as the molar ratio of S1 to actin increased and was saturated at a molar ratio of less than 1.0 in the presence of Ca^{2+}. Assuming that all thin filaments are in the S1-induced state at the molar ratio of 1, the distances between Cys-60 or Cys-250 of TnT and Cys-374 of F-actin on mutant thin filaments in the S1-induced state were 41.8 ± 0.9 and 45.3 ± 1.1 Å, respectively. S1-rigor binding increased the distance between Cys-60 or Cys-250 of TnT and Cys-374 of F-actin by ~9 Å in the presence of Ca^{2+}. In the absence of Ca^{2+}, the extent of the S1-induced conformational change also increased as the molar ratio of S1 to actin increased, and the relative fluorescence intensities (1 – *E*) at the molar ratio of 1 were close to those in the presence of Ca^{2+}.

The effects of S1 binding on FRET between AEDANS-60- or AEDANS-250-Tn and FLC-F-actin were also measured under the same experimental conditions as DAB-F-actin, except that fluorescence intensity was measured at 460 nm instead of 490 nm in order to avoid the contribution of the acceptor-fluorescence from FLC (Fig. 5). The extent of the S1-induced conformational change increased as the molar ratio of S1 increased in both the presence and ab-sence of Ca^{2+} in the same way as the case of DAB-F-actin. S1-rigor binding increased the distance between Cys-60 of TnT and Gln-41 of F-actin further by ~8 Å and the distance between Cys-250 of TnT and Gln-41 of F-actin by ~6 Å in the pres-

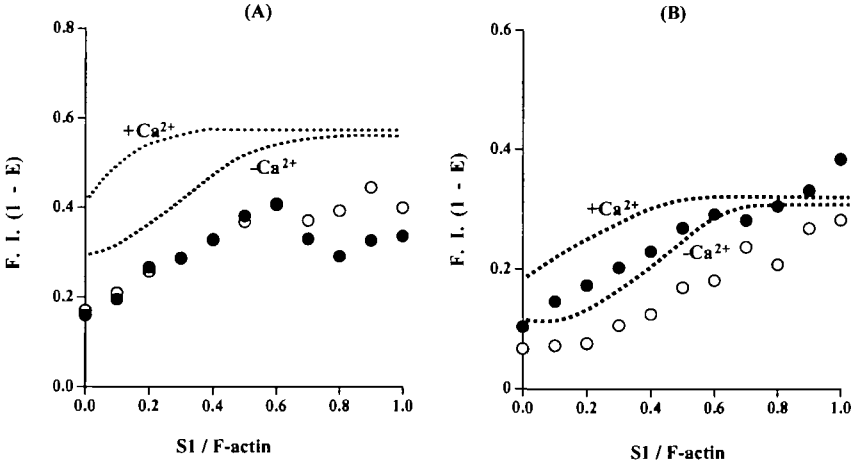

Fig. 5. **Relative fluorescence intensities (1 - *E*) of AEDANS bound to Cys-60 (A) and Cys-250 (B) of TnT on mutant thin filaments *vs.* molar ratios of S1 to actin. Resonance energy acceptor was FLC, which was attached to Gln-41 of actin.** Values were obtained in buffer F and 50 μM $CaCl_2$ for the $+Ca^{2+}$ state (●) or 1 mM EGTA for the $-Ca^{2+}$ state (○) at 20°C. The data were corrected by the same calculation as in Fig. 4. Concentrations of F-actin, D234Tm, and Tn were 0.23, 0.044, and 0.042 mg/ml, respectively. Fluorescence measurements were carried out after hydrolysis of contaminant ATP (less than 10 μM). Excitation was at 340 nm and emission was measured at 460 nm. Broken lines are the transition curves with wild-type thin filaments instead of mutant thin filaments measured in the preceding paper (*17*).

TABLE I. **Distances between probes attached to Tn and actin in the thin filament reconstituted with D234Tm in the presence and absence of Ca^{2+} ions and S1.** The values in parenthesis are cited from Ref. *17* and were obtained in the thin filament reconstituted with native Tm.

Donor site (Tn)	Acceptor site (F-actin)		Ca^{2+}	R_0 (2/3) (Å)	Efficiency	R (2/3) (Å) on D234Tm	R (2/3) (Å) on native Tm
TnT60	Gln-41		+	44.3	0.82 ± 0.01	34.2 ± 0.4	(42.1 ± 0.6)
			–				(39.5 ± 0.3)
		+S1	+	44.3	0.57 ± 0.03	42.2 ± 0.9	45.7 ± 1.0
			–				46.7 ± 1.0
	Cys-374		+	37.9	0.70 ± 0.01	33.0 ± 0.3	(34.4 ± 0.2)
			–				(30.8 ± 0.3)
		+S1	+	37.9	0.36 ± 0.03	41.8 ± 0.9	38.9 ± 0.8
			–				39.7 ± 0.8
TnT250	Gln-41		+	45.6	0.85 ± 0.01	34.2 ± 0.5	(35.8 ± 0.8)
			–	46.3	0.90 ± 0.01	31.9 ± 0.6	(30.0 ± 0.8)
		+S1	+	45.6	0.68 ± 0.02	40.1 ± 0.6	40.9 ± 0.9
			–	46.3	0.73 ± 0.02	39.4 ± 0.7	40.9 ± 1.0
	Cys-374		+	38.9	0.60 ± 0.01	36.4 ± 0.3	(36.6 ± 0.2)
			–	39.4	0.79 ± 0.02	31.5 ± 0.6	(29.6 ± 0.4)
		+S1	+	38.9	0.29 ± 0.03	45.3 ± 1.1	41.0 ± 0.7
			–	39.4		45.9 ± 1.1	39.4 ± 0.7

ence of Ca^{2+}. In the absence of Ca^{2+}, the relative fluorescence intensities ($1 - E$) at the molar ratio of 1 were close to those in the presence of Ca^{2+}.

It should be emphasized here that curves of the S1-induced conformational change for AEDANS-60-Tn on mutant thin filaments were distinctly sigmoidal irrespective of Ca^{2+} concentration, although the curve on wild-type thin filaments was hyperbolic in the presence and sigmoidal in the absence of Ca^{2+} (*17*).

The transfer efficiencies and distances in the present FRET measurements are summarized in Table I.

DISCUSSION

Recent kinetic studies have provided evidence for a model in which a thin filament exists in one of three states: a blocked state, in which muscle is relaxed; a closed state, which is induced by Ca^{2+} binding to Tn; and an open state, which is induced by strong S1 binding (*22, 23*). 3D-EM studies have analyzed the Ca^{2+}-induced conformational change of thin filaments as a Tm movement towards the outer domain of actin molecule, which exposes several additional myosin-binding sites on actin, thereby strongly promoting hydrophobic binding of actin to myosin [see review (*24*)]. However, FRET measurements did not detect any significant movement of Tm (*8, 9, 14, 25, 26*). On the other hand, FRET between probes attached to TnI and actin demonstrated that TnI moves substantially on thin filaments in response to changes in Ca^{2+} concentration (*9–14*). Furthermore, FRET measurements between probes attached to Cys-60 or Cys-250 of TnT and Gln-41 or Cys-374 of actin demonstrated that not only TnI but also TnT showed a substantial Ca^{2+}-induced mass movement on thin filaments (*17*).

3D-EM studies have also analyzed the S1-induced conformational change of thin filaments as a further Tm movement towards the outer domain of actin, resulting in the exposure of additional myosin binding sites on actin. Consequently, an active interaction between actin and myosin is available (*27, 28*). Similar conclusions about Ca^{2+}- and S1-induced movements of Tm have been deduced from X-ray diffraction studies of skinned rabbit skeletal muscle fibers and oriented actin-Tm filaments (*29*). However, FRET measurements did not detect any S1-induced movement of Tm on thin filaments (*14*). On the other hand, FRET demonstrated that rigor S1 binding to actin induces a significant movement of TnI on the reconstituted thin filament (*13, 14*). FRET also demonstrated a significant S1-induced movement of TnT on reconstituted thin filaments (*17*). When the filaments were fully decorated with S1, TnI and TnT moved to the same positions on reconstituted thin filaments in the absence of Ca^{2+} as in the presence of Ca^{2+} (*14, 17*). Plots of the extent of S1-induced conformational change *vs.* molar ratio of S1 to actin showed that the curves for both TnI and TnT in the presence of Ca^{2+} are hyperbolic, while in the absence of Ca^{2+}, the curves for both TnI and TnT are sigmoidal.

The previous FRET measurement (*14*) showed almost the same Ca^{2+}-induced movement of TnI on mutant thin filaments as on wild-type thin filaments. However, plots of the extent of S1-induced TnI-movement *vs.* molar ratio of S1 to actin showed that the curve for mutant thin filaments is sigmoidal irrespective of Ca^{2+} concentration, whereas that for wild-type thin filament is hyperbolic in the presence of Ca^{2+} and sigmoidal in the absence of Ca^{2+}. The results provided structural evidence for three states of thin filaments in the regulation mechanism of skeletal muscle contraction and showed that the transition from the closed state to the open state is severely impaired on mutant thin filaments. However, it was not clear why the transition was severely impaired, since the Ca^{2+}-induced movement of TnI seemed normal. The present FRET measurements showed that, in contrast to TnI, the Ca^{2+}-induced movement of TnT on mutant thin filaments was severely impaired, although TnT on wild-type thin filaments demonstrated substantial Ca^{2+}-induced movement. The N-terminal region (Cys-60) of TnT did not show any appreciable Ca^{2+}-induced movement on mutant thin filaments. On the other hand, the C-terminal region (Cys-250) of TnT showed some Ca^{2+}-induced movement on mutant thin filaments, but much less than that on wild-type thin filaments. TnT extends along the C-terminal third of Tm, and the N-terminus of TnT binds to the head-to-tail overlap region of two adjacent Tm molecules (*3*). TnI and TnC form a globular portion of Tn and bind to the C-terminal region of TnT. The C-terminal region of TnT interacts with N-terminal region of TnI (*5, 30*). TnI showed the same extent of Ca^{2+}-induced movement on mutant thin filaments as on wild-type thin filaments (*14*). The C-terminal region of TnT seems to move in company with TnI, but the movement of the C-terminal region of TnT on mutant thin filaments is not sufficient to induce the subsequent movement of the N-terminal region. The C-terminal region of TnT has a Ca^{2+}-dependent Tm-binding site. The C-terminal 17 residues of TnT2 contain a Tm-binding site that is critical for the Ca^{2+}-sensitizing activity of TnT (*31*). Cys-250 of TnT is localized near this Tm-binding site. D234Tm may lack the binding site for the C-terminal region of TnT. The globular portion of the troponin complex is located near residues 150–180 on Tm (*2*). D234Tm, in which amino acid residues 49–167 are deleted, lacks a part of this Tn globular portion-binding region. This region of Tm (amino acid residues 150–167) may be important for Ca^{2+}-dependent TnT binding. Upon Ca^{2+} binding to TnC, TnI moves properly away from the outer domain of actin, but the C-terminal region of TnT does not bind properly to D234Tm, which causes the lack of movement of the N-terminal region of TnT. This may explain why the Ca^{2+}-induced movement of TnT is impaired on mutant thin filaments.

The present FRET measurements showed that TnT also changed position on mutant thin filaments upon rigor S1 binding. The distances between Cys-374 of F-actin and Cys-60 or Cys-250 of TnT increased by 9 Å when the filaments were fully saturated with rigor S1, and the distances between Gln-41 of F-actin and Cys-60 or Cys-250 of TnT increased by 6 or 8 Å, respectively. In the case of FRET between Cys-60 of TnT and Cys-374 of actin, plots of S1-induced change *vs.* molar ratio of S1 to actin on mutant thin filaments showed sigmoidal curves irrespective of Ca^{2+} concentration (in Fig. 4a). On the other hand, the curve on wild-type thin filaments was hyperbolic in the presence of Ca^{2+} and sigmoidal in the absence of Ca^{2+}. These tendencies of the transition curves were seen in the case of S1-induced TnI movement on wild-type and mutant thin filaments (*14*). On the other hand, in the case of FRET between Cys-250 of TnT and Cys-374 of actin, the transition curve was

sigmoidal in the absence of Ca^{2+} but hyperbolic in the presence of Ca^{2+} (in Fig. 4b), as seen on wild-type thin filaments. The TnT subunit moved on the thin filaments not as a solid rod but as a flexible rod upon strong S1 binding. Upon Ca^{2+} binding to TnC, TnI moves away from the outer domain of actin to interact with TnC, and the C-terminal region of TnT also moves, even on mutant thin filaments. However, this movement of the C-terminal region of TnT is not large enough to induce movement of the N-terminal region of TnT on mutant thin filaments. For the movements of the N-terminal region of TnT and also TnI on mutant thin filaments, simultaneous binding of several rigor S1 molecules on the unit length of a mutant thin filament is required even in the presence of Ca^{2+}. These movements correspond well to three states of thin filaments.

It should be mentioned here that 3D-EM failed to detect any structural difference in the Ca^{2+}-induced state between thin filaments reconstituted with full-length Tm and those reconstituted with D234Tm (*16*). On the other hand, FRET clearly detected the deficiency of the Ca^{2+}-induced TnT-movement on mutant thin filaments in contrast to wild-type thin filaments. Furthermore, 3D-EM failed to detect any structural difference in the S1-induced state between wild-type and mutant thin filaments, but FRET clearly showed the significant difference in the transition curves from the closed state to the open state between wild-type and mutant thin filaments. These structural differences may be responsible for the functional deficiency in D234Tm. The resolution of 3D-EM for thin filaments is limited to ~35 Å without imposing helical symmetry (*32*), while the resolution of FRET is within several Å. Furthermore, the identification of conformational changes is straight in FRET but not in 3D-EM. Thus, FRET is very useful for detecting conformational changes of proteins. From FRET measurements we concluded that movement of Tn, but not Tm, is critical for muscle regulation in accordance with our regulation model (*8, 14, 17, 33*).

We wish to thank the Food Research and Development Laboratories of Ajinomoto Co. for the generous gift of microbial transglutaminase.

REFERENCES

1. Ebashi, S., Endo, M., and Ohtsuki, I. (1969) Control of muscle contraction. *Q. Rev. Biophys.* **2**, 351–384
2. White, S.P., Cohen, C., and Phillips Jr, G.N. (1987) Structure of co-crystals of tropomyosin and troponin. *Nature* **325**, 826–828
3. Ohtsuki, I., Maruyama, K., and Ebashi, S. (1986) Regulatory and cytoskeletal proteins of vertebrate skeletal muscle. *Adv. Protein Chem.* **38**, 1–67
4. Gordon, A.M., Homsher, E., and Regnier, M. (2000) Regulation of contraction in striated muscle. *Physiol. Rev.* **80**, 853–924
5. Farah, C.S. and Reinach, F.C. (1995) The troponin complex and regulation of muscle contraction. *FASEB J.* **9**, 755–767
6. dos Remedios, C.G., Miki, M., and Barden, J.A. (1987) Fluorescence resonance energy transfer measurements of distances in actin and myosin. A critical evaluation. *J. Muscle Res. Cell Motil.* **8**, 97–117
7. Miki, M., O'Donoghue, S.I., and dos Remedios, C.G. (1992) Structure of actin observed by fluorescence resonance energy transfer spectroscopy. *J. Muscle Res. Cell Motil.* **13**, 132–145
8. Miki, M., Miura, T., Sano, K., Kimura, H., Kondo, H., Ishida, H., and Maéda, Y. (1998) Fluorescence resonance energy transfer between points on tropomyosin and actin in skeletal muscle thin filaments: Does tropomyosin move? *J. Biochem.* **123**, 1104–1111
9. Miki, M. (1990) Resonance energy transfer between points in a reconstituted skeletal muscle thin filament: A conformational change of the thin filament in response to a change in Ca^{2+} concentration. *Eur. J. Biochem.* **187**, 155–162
10. Tao, T., Gong, B.J., and Leavis, P.C. (1990) Calcium-induced movement of troponin-I relative to actin in skeletal muscle thin filaments. *Science* **247**, 1339–1341
11. Miki, M. and Iio, T. (1993) Kinetics of structural changes of reconstituted skeletal muscle thin filaments observed by fluorescence resonance energy transfer. *J. Biol. Chem.* **268**, 7101–7106
12. Miki, M., Kobayashi, T., Kimura, H., Hagiwara, A., Hai, H., and Maéda, Y. (1998) Ca^{2+}-induced distance change between points on actin and troponin in skeletal muscle thin filaments estimated by fluorescence resonance energy transfer spectroscopy. *J. Biochem.* **123**, 324–331
13. Kobayashi, T., Kobayashi, M., and Collins, J.H. (2001) Ca^{2+}-dependent, myosin subfragment 1-induced proximity changes between actin and the inhibitory region of troponin I. *Biochim. Biophys. Acta* **1549**, 148–154
14. Hai, H., Sano, K., Maeda, K., Maéda Y., and Miki, M. (2002) Ca^{2+}-induced conformational change of reconstituted skeletal muscle thin filaments with an internal deletion mutant D234-tropomyosin observed by fluorescence energy transfer spectroscopy: structural evidence for three states of thin filament. *J. Biochem.* **131**, 407–418
15. Landis, C.A., Bobkova, A., Homsher, E., and Tobacman, L.S. (1997) The active state of the thin filament is destabilized by an internal deletion in tropomyosin. *J. Biol. Chem.* **272**, 14051–14056
16. Rosol, M., Lehman, W., Craig, R., Landis, C., Butters, C., and Tobacman, L.S. (2000) Three-dimensional reconstruction of thin filaments containing mutant tropomyosin. *Biophys. J.* **78**, 908–917
17. Kimura, C., Maeda, K., Maéda, Y., and Miki, M. (2002) Ca^{2+}- and S1-induced movement of Troponin T on reconstituted skeletal muscle thin filaments observed by fluorescence energy transfer spectroscopy. *J. Biochem.* **132**, 93–102
18. Lamkin, M., Tao, T., and Lehrer, S.S. (1983) Tropomyosin-troponin and tropomyosin-actin interactions: a fluorescence quenching study. *Biochemistry* **22**, 3053–3058
19. Lorand, L., Parameswaran, K.N., Velasco, P.T., Hsu, L.K.-H., and Siefring, G.E., Jr. (1983) New colored and fluorescent amine substrates for activated fibrin stabilizing factor (Factor XIIIa) and for transglutaminase. *Anal. Biochem.* **131**, 419–425
20. Hudson, E.N. and Weber, G. (1973) Synthesis and characterization of two fluorescent sulfhydryl reagents. *Biochemistry* **12**, 4154–4161
21. Scott, T.G., Spencer, R.D., Leonard, N.G., and Weber, G. (1970) Emission properties of NADH. Studies of fluorescence lifetimes and quantum efficiencies of NADH, AcPyADH, and simplified synthetic models. *J. Am. Chem. Soc.* **92**, 687–695
22. Mckillop, D.F. and Geeves, M.A. (1993) Regulation of the interaction between actin and myosin subfragment 1: evidence for three states of the thin filament. *Biophys. J.* **65**, 693–701
23. Lehrer, S.S. and Geeves, M.A. (1998) The muscle thin filament as a classical cooperative/allosteric regulatory system. *J. Mol. Biol.* **277**, 1081–1089
24. Amos, L.A. (1985) Structure of muscle filaments studied by electron microscopy. *Annu. Rev. Biophys. Biophys. Chem.* **14**, 291–313
25. Miki, M. and Mihashi, K. (1979) Conformational changes of reconstituted thin filament under the influence of Ca^{2+} ion-Fluorescence energy transfer and anisotropy decay measurements (in Japanese). *Seibutsu-Butsuri* **19**, 135–140
26. Tao, T., Lamkin, M., and Lehrer, S.S. (1983) Excitation energy transfer studies of the proximity between tropomyosin and actin in reconstituted skeletal muscle thin filaments. *Biochemistry* **22**, 3059–3066
27. Vibert, P., Craig, R., and Lehman, W. (1997) Steric-model for activation of muscle thin filamenents. *J. Mol. Biol.* **266**, 8–14
28. Xu, C., Craig, R., Tobacman, L., Horowitz, R., and Lehman, W.

(1999) Tropomyosin positions in regulated thin filaments revealed by cryoelectron microscopy. *Biophys. J.* **77**, 985–992
29. Holmes, K.C. (1995) The actomyosin interaction and its control by tropomyosin. *Biophys. J.* **68** (suppl.), 2–7
30. Stefancsik, R., Jha, P.K., and Sarker, S. (1998) Identification and mutagenesis of a highly conserved domain in troponin T responsible for troponin I binding: potential role for coiled coil interaction. *Proc. Natl. Acad. Sci. USA* **95**, 957–962
31. Onoyama, Y. and Ohtsuki, I. (1986) Effect of chymotryptic troponin T subfragments on the calcium ion-sensitivity of ATPase and superprecipitation of actomyosin. *J. Biochem.* **100**, 517–519
32. Narita, A., Yasunaga, T., Ishikawa, T., Mayanagi, K., and Wakabayashi, T. (2001) Ca^{2+}-induced switching of troponin and tropomyosin on actin filaments as revealed by electron cryomicroscopy. *J. Mol. Biol.* **308**, 241–261
33. Miki, M. (2002) Structural changes between regulatory proteins and actin: A regulation model by tropomyosin-troponin based on FRET measurements in *Molecular Interactions of Actin*, Vol. 2 (Thomas, D.D. and dos Remedios, C.G., eds.) pp. 191–203, Springer Verlag, Heidelberg